New A-F type pulsating variable stars

Ö. Kırmızıtaş,[1,*] S. Çavuş,[1] and F. Kahraman Aliçavuş[1,2]

[1] *Çanakkale Onsekiz Mart University, Faculty of Sciences and Arts, Physics Department, 17100, Canakkale, Turkey*

[2] *Çanakkale Onsekiz Mart University, Astrophysics Research Center and Ulupınar Observatory, TR-17100, Çanakkale, Turkey*

Pulsating stars are remarkable objects for stellar astrophysics. Their pulsation frequencies allow us to probe the internal structure of stars. One of the most known groups of pulsating stars is δ Scuti variables which could be used to understand the energy transfer mechanism in A-F type stars. Therefore, in the current study, we focused on the discovery of δ Scuti stars. For this investigation, we chose some of these stars by following some criteria. First, we inspected TESS database by eye and discovered some stars that exhibit pulsation like behaviour. Our second criterion is $T_{\rm eff}$ and $\log g$ range. The δ Scuti stars generally have $T_{\rm eff}$ and $\log g$ value in a range of $6300-8500$ K and $3.2-4.3$, respectively. Hence, we selected the stars with TIC $T_{\rm eff}$ and $\log g$ in these ranges. The other criterion is the pulsating frequency. A frequency analysis was performed for all stars in the candidate list. In addition, M_V, L and also M_{bol} parameters of the target stars were determined to calculate the pulsation constants and show the position of the stars on the H-R diagram. The final pulsation type classification was made by considering the frequency ranges and pulsation constants of the stars. As a result of the study, five δ Scuti, one γ Doradus and four hybrid systems were discovered.

Keywords: stars: pulsating—stars: delta Scuti Variable Stars, Pulsating Variable Stars, Delta Scuti Stars, Transit Exoplanet Survey Satellite (TESS) Satellite.

1. INTRODUCTION

Asteroseismology is a great tool to investigate interior structure of stars via their oscillation modes. The main targets of asteroseismology is the pulsating variables. There are many pulsating stars known for decades such as β Cephei, δ Scuti and Cepheid stars. Inside the group of pulsating variables, the main sequence A-F type oscillating stars occupy a significant place in asteroseismology, as they are located on transition region where the convection envelopes of stars turn into radiative envelope (Aerts, Christensen-Dalsgaard, & Kurtz 2010). To understand the mechanism operating in that region, investigations of these A-F type pulsating stars become very important.

Mainly, there are two main-sequence A-F type pulsating variables; δ Scuti (δ Sct) and γ Doradus (γ Dor) stars. The δ Sct stars have a spectral type of A0-F5 with luminosity class changing from dwarf to giant (Chang et al. 2013). These variables exhibit radial and non-radial oscillations with a general frequency range of $5-50\,{\rm d}^{-1}$ (Aerts, Christensen-Dalsgaard, & Kurtz 2010, Breger 2000). The γ Dor stars are dwarf and/or sub-dwarf variables with a spectral type of A7-F5 (Kaye et al. 1999). These variables exhibit non-radial pulsations with a frequency generally lower than $5\,{\rm d}^{-1}$ (Kaye et al. 1999, Uytterhoeven et al. 2011). The instability strips of these A-F type pulsating stars are place the lower part of the classical instability strip and they are partially overlap. In this overlapping part, existence of δ Sct and γ Dor hybrid stars was proposed (Breger & Beichbuchner 1996, Dupret et al. 2004, Handler & Shobbrook 2002). These hybrid variables may also be called A-F type hybrids. These stars show both δ Sct and γ Dor type oscillations at the same time.

A great revolution on the study of A-F type pulsating variables have been achieved by the contribution of space telescopes. Especially, studies of high-quality *Kepler* (Borucki et al. 2010) data had a significant contribution. Uytterhoeven et al. (2011) were examined *Kepler* data of 750 A-F type pulsating stars and revealed a general information about these variables and

* ozlemkirmizitas1907@gmail.com

Table 1. Information about the targets. The parameters were taken from TIC (Stassun et al. 2019).

TIC	TESS mag ± 0.006	$T_{\rm eff}$ (K) ± 136	$\log g$ ± 0.08	TESS Sectors
25537276	8.52	6866	3.36	16
177422294	8.48	7223	3.34	17
252554307	8.46	6812	3.81	16
279874050	8.20	6873		17, 18, 24, 25
308447073	8.74	7539	4.29	18
367910480	5.87	8476	4.03	18, 19, 24, 25
370599803	8.09	7394	3.76	18
395520454	8.88	7353		25
400502366	8.15	8261	3.54	18
431375592	8.72	6411	4.04	16, 17

also show that there are some unexpected situations about these pulsators. For example, they showed that some δ Sct, γ Dor and/or hybrid stars may place outside of theoretically suggested area. This situation is not expected according to the theoretical studies (Dupret et al. 2004, 2005).

After *Kepler*, Transiting Exoplanet Survey Satellite (TESS, Ricker et al. (2015)) started to provide high-quality space data of many stellar systems. The first study of A-F type pulsating stars with TESS data was presented by Antoci et al. (2019) and properties of these variables were examined. As the TESS almost observed the entire sky, it is a significant tool to investigate these kinds of variables and discover new candidates. Therefore in this study we present one part of our TESS field search to revel some new A-F type pulsating stars. The paper is organized as follows. Information about used TESS data and the criteria of target selection are given in Sect. 2. The time-series analysis is present in Sect. 3. Discussion and conclusions are introduced in Sect. 4.

2. DATA AND TARGET SELECTION

In this study, TESS data were used for discovering new A-F type pulsating variables. The main mission of TESS is detecting new exoplanets orbiting around close stars (Ricker et al. 2015). TESS was launched from Cape Canaveral Base in the USA on April 2018, with the Falcon 9 rocket produced by SpaceX company. TESS has the same working logic with the *Kepler* space telescope, however, it scans a wider area. TESS satellite has four identical CCD cameras and each has a 24×24 degree field of view (Ricker et al. 2015). Both the Northern and Southern hemispheres have been observed by TESS and it has provided many data of stellar systems in addition to revealing new exoplanets (e.g. Antoci et al. 2019). TESS photometric data has been obtained in 2-min short (SC) and 30-mins long (LC) cadences during first two years mission. Those data are released in the Barbara A. Mikulski Archive for Telescopes (MAST)[1] archive.

In the current study, we present a part of our Northern TESS filed research to discover unknown δ Scuti type variables. We took the TESS data from MAST archive. Only SC TESS data were checked to find these kinds of variable stars. First criterion in our target selection is determining some stars showing pulsating like variation in their light curve. In this study we only focused on single pulsating variables and eliminated the eclipsing binaries. The second criterion is the effective temperature ($T_{\rm eff}$) and also surface gravity ($\log g$) range. δ Scuti stars have generally $T_{\rm eff}$ and $\log g$ in the range of 6300 - 8500 K and 3.2 - 4.3 (Rodríguez & Breger 2001), so we controlled these values of the systems found in the first target selection. The $T_{\rm eff}$ and $\log g$ values of the selected systems were checked from the TESS Input Catalog (Stassun et al. 2019). The stars having $T_{\rm eff}$ values in the given $T_{\rm eff}$ range were chosen as a result of this target selection criterion. The final criterion is determining the unknown systems in the literature. Therefore as a final step we checked the literature information of the stars found in the previous selection parts

[1] https://mast.stsci.edu

and determined the unknown systems. The final target list was obtained by considering these three criteria. This list is given in Table 1.

To confirm the pulsational variability of the selected systems one needs to analyse TESS data in detail. Therefore, all SC TESS data of the systems were collected. The SAP fluxes were taken into account and these data were converted into magnitude. The final TESS data were also normalised by using a polynomial fit to eliminate possible instrumental effects.

3. FREQUENCY ANALYSIS

To reveal the pulsation characteristic of the selected targets a frequency analysis was performed. In the frequency analysis, all available SC data of the systems were used because the Nyquist frequency of SC data reach to $\sim$360 d^{-1}. Considering the pulsation period range of the δ Scuti stars, the SC data are suitable to searching for δ Scuti-type oscillations. In the frequency analysis, the Period04 program (Lenz & Breger 2005) was used. Basing on the Fourier and nonlinear least square fitting the program searches for single and multiple frequencies with the "prewhitening" method (Handler 2009). The program is also convenient to detect possible harmonic and combination frequencies.

According to the criterion given by Breger et al. (1993), the frequencies having a signal-to-noise (S/N) ratio over 4 is considered as significant. However, in a recent study of Baran & Koen (2021), it was showed that for the space-based TESS data S/N ratio should be higher than typically used Breger criterion to detect significant frequencies. Therefore, taking into account the results of this study we considered the frequencies as significant if they have S/N ratio over 4.5.

As a result of the frequency analysis, we derived the pulsation frequencies of the targets and list the first ten frequencies and their S/N ratios in Table 1. In this table, harmonic and combination frequencies are not listed. The full list of the frequencies is given in an electronic form. The Fourier spectra of the target stars are shown in Fig. 1.

4. DISCUSSION AND CONCLUSIONS

In this study, we present the analysis of some TESS field A-F type stars and revealed their pulsational characteristics. We selected the systems from the TESS field with inspection by eye and considering the some criteria such as $T_{\rm eff}$, frequency range.

First, a frequency analysis was performed and all significant frequencies of the targets were derived. To classify the pulsation type of the system, we also calculated the pulsation constant and examine their position on the Hertzsprung-Russell (H-R) diagram. To do this, some important parameters of the targets were obtained. The extinction coefficient (A_v) was determined by using the galactic extinction map (Amôres & Lépine 2005) with the help of the galactic coordinates and the Gaia eDR3 parallaxes (Gaia Collaboration et al. 2021) of the targets. The calculated coefficients were then used to derive absolute magnitude (M_V), luminosity (L) and also bolometric magnitude (M_{bol}) with the same way described in the study of Poro et al. (2021). The calculated parameters are given in Table 2.

The resulting parameters were used to obtain the pulsation constant. Pulsation constant (Q) is defined by the following formula:

$$Q = P\sqrt{\frac{\bar{\rho}}{\bar{\rho}_{\odot}}}$$

This equation can also be given as described by Breger (1990),

$$\log(Q/P) = 0.5 \log g + 0.1 M_{bol} + \log T_{\rm eff} - 6.456$$

In our study, the Q values of the target stars were calculated using the above equation and the parameters given in Table 1 and Table 2. For some stars there are no $\log g$ parameters. For these stars we assumed the $\log g$ as 4.0. The range of the calculated Q values for each star is given in Table 2. By taking into account the frequency spectra and the Q values of the targets we made final pulsation classification. The Q constant is different for the δ Sct and γ Dor stars. In the study of Handler & Shobbrook (2002), they presented the Q distribution for both pulsating

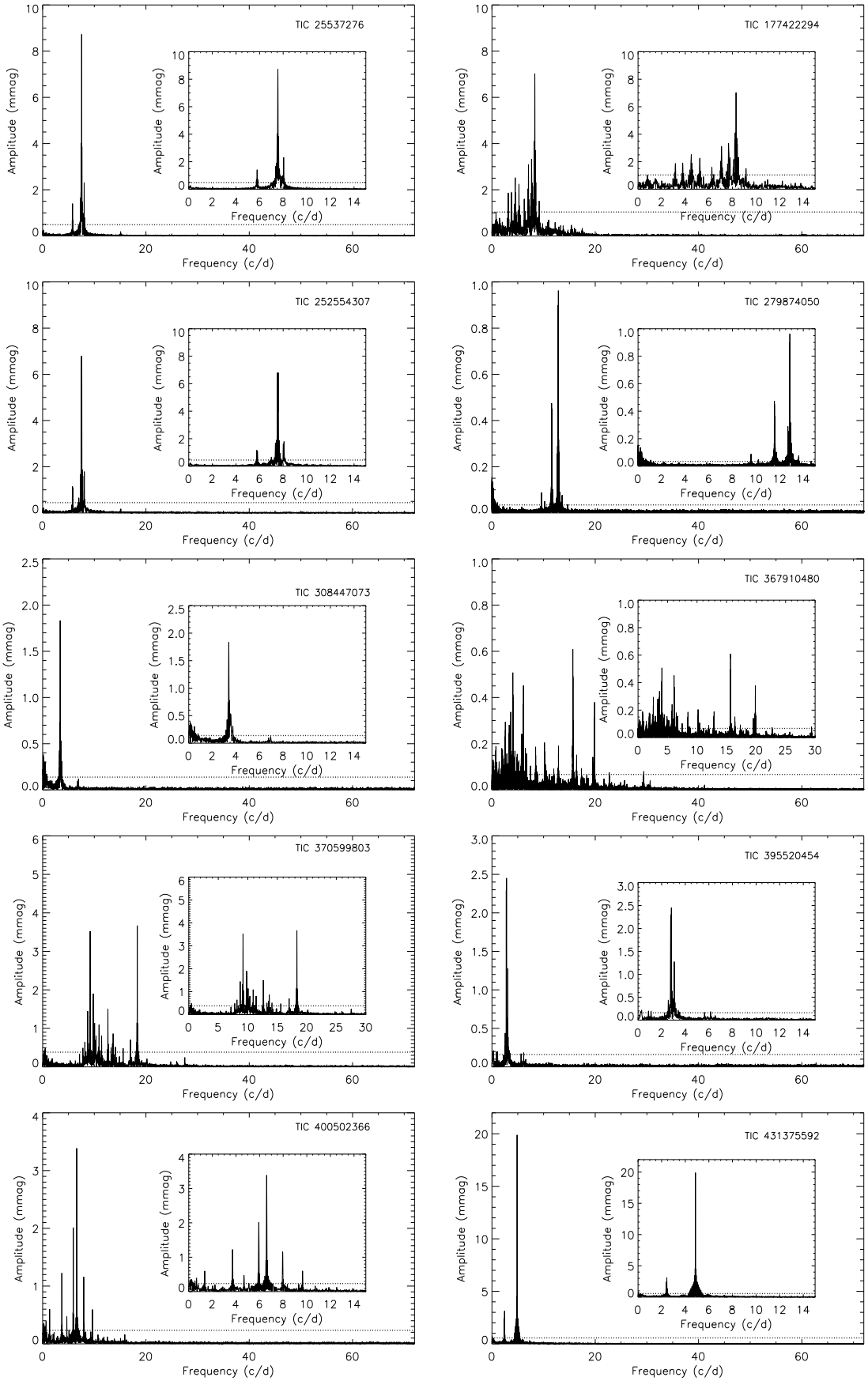

Figure 1. Fourier spectra of the target stars. Dotted lines represent the 4.5-σ level.

Table 2. Derived parameters for the targets and classification.

	TIC number	A_v (mag) ± 0.002	M_V (mag)	M_{bol} (mag)	log $(L/L_\odot)$	Q range	Classification
1	25537276	0.08476	0.906 ± 0.013	0.987 ± 0.014	1.562 ± 0.033	$0.011 - 0.025$	δ Scuti
2	177422294	0.09086	0.615 ± 0.013	0.690 ± 0.014	1.678 ± 0.033	$0.017 - 0.037$	δ Scuti
3	252554307	0.04787	2.149 ± 0.011	$2.229 \pm 0{,}012$	1.065 ± 0.031	$0.021 - 0.056$	δ Scuti
4	279874050	0.04848	1.713 ± 0.026	$1.794 \pm 0{,}027$	1.239 ± 0.046	$0.028 - 0.031$	δ Scuti
5	308447073	0.03920	2.631 ± 0.022	2.690 ± 0.023	0.872 ± 0.042	$0.192 - 0.212$	γ Doradus
6	367910480	0.00000	1.301 ± 0.010	1.273 ± 0.011	1.403 ± 0.030	$0.021 - 0.161$	Hybrid
7	370599803	0.06602	1.463 ± 0.013	1.530 ± 0.014	1.339 ± 0.033	$0.015 - 0.029$	δ Scuti
8	395520454	0.06427	2.539 ± 0.025	2.608 ± 0.026	0.909 ± 0.045	$0.050 - 0.120$	Hybrid
9	400502366	0.16216	0.276 ± 0.014	0.273 ± 0.015	1.814 ± 0.034	$0.032 - 0.465$	Hybrid
10	431375592	0.03094	3.189 ± 0.011	3.255 ± 0.012	0.648 ± 0.031	$0.103 - 0.211$	Hybrid

star types. For δ Sct and γ Dor stars, the Q is in the range of $\sim 0.008 - 0.063$ and $0.200 - 1.260$, respectively. Considering these Q values and the frequency spectra we classified the stars. The final classification is given in the Table 2. As a result of these investigation, we determined five δ Sct, one γ Dor and four hybrid stars. The position of stars are shown on the H-R diagram as well. As can be seen from Fig. 2, the δ Sct star are located inside their instability strip and also γ Dor variable is placed very close its own domain. However, the hybrid stars are mostly located outside of both instability strips. This result is excepted for these variable stars according to the result found by Uytterhoeven et al. (2011). There are a few hypnotises to explain the existence of these variables such as wrong $T_{\rm eff}$, fast rotation and binarity (Lampens et al. 2018, 2020). No certain explanation has been found yet. As s result of this study, we revealed ten A-F type pulsating stars which was not known in the literature before.

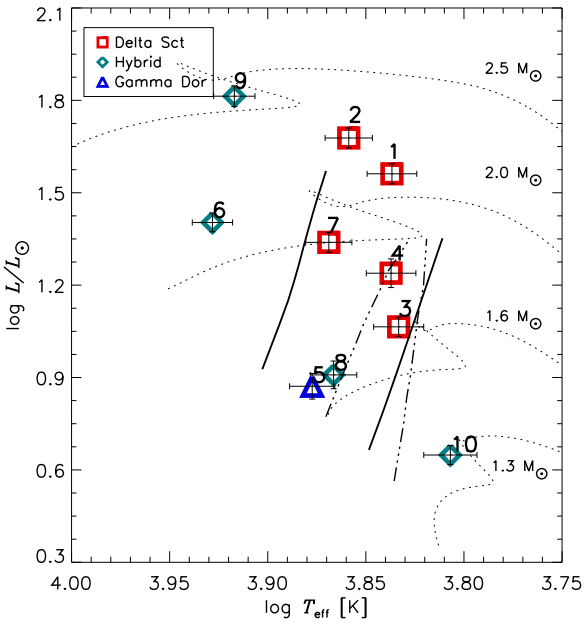

Figure 2. Position of the targets in the H-R diagram.The numbers are the same given in Table 1. The solid and dot-dash lines represent the instability strips of δ Sct and γ Dor stars respectively (Dupret et al. 2005). The dot lines are the evolutionary tracks taken from Kahraman Aliçavuş et al. (2016).

ACKNOWLEDGMENTS

This study has been supported by the Scientific and Technological Research Council (TUBITAK) project through 120F330. The TESS data presented in this paper were obtained from the Mikulski Archive for Space Telescopes (MAST). Funding for the TESS mission is provided by the NASA Explorer Program. This work has made use of data from the European Space Agency (ESA) mission Gaia (http://www.cosmos.esa.int/gaia), processed by the Gaia Data Processing and Analysis Consortium (DPAC, http://www.cosmos.esa.int/web/gaia/dpac/consortium). Funding for the DPAC has been provided by national institutions, in particular the institutions participating in the Gaia Multilateral Agreement. This research has made use of the SIMBAD data base, operated at CDS, Strasbourq, France.

FUNDING

This study has been supported by the Scientific and Technological Research Council (TUBITAK) project through 120F330.. . .

CONFLICT OF INTEREST

The authors declare no conflicts of interest.

REFERENCES

Aerts C., Christensen-Dalsgaard J., Kurtz D. W., 2010, *Astroseismology*, Springer, Berlin

Amôres E. B., Lépine J. R. D., 2005, AJ, 130, 659

Antoci, V., Cunha, M. S., Bowman, D. M., et al. 2019, Monthly Notices Royal Astron. Soc. , 490, 4040. doi:10.1093/mnras/stz2787

Baran A. S., Koen C., 2021, AcA, 71, 113. doi:10.32023/0001-5237/71.2.3

Breger M., 1990, DSSN, 2

Breger M., Stich J., Garrido R., Martin B., Jiang S.-Y., Li Z.-P., Hube D. P., et al., 1993, A&A, 271, 482

Breger M., Beichbuchner F., 1996, A&A, 313, 851

Breger M., 2000, ASPC, 210, 3

Borucki W. J., Koch D., Basri G., Batalha N., Brown T., Caldwell D., Caldwell J., et al., 2010, Sci, 327, 977. doi:10.1126/science.1185402

Chang S.-W., Protopapas P., Kim D.-W., Byun Y.-I., 2013, AJ, 145, 132

Dupret M.-A., Grigahcène A., Garrido R., Gabriel M., Scuflaire R., 2004, A&A, 414, L17

Dupret M.-A., Grigahcène A., Garrido R., Gabriel M., Scuflaire R., 2005, A&A, 435, 927

Gaia Collaboration, Smart R. L., Sarro L. M., Rybizki J., Reylé C., Robin A. C., Hambly N. C., et al., 2021, A&A, 649, A6. doi:10.1051/0004-6361/202039498

Handler G., Shobbrook R. R., 2002, MNRAS, 333, 251

Handler, G. 2009, Monthly Notices Royal Astron. Soc. , 398, 1339. doi:10.1111/j.1365-2966.2009.15005.x

Kahraman Aliçavuş F., Niemczura E., De Cat P., Soydugan E., Kołaczkowski Z., Ostrowski J., Telting J. H., et al., 2016, MNRAS, 458, 2307. doi:10.1093/mnras/stw393

Kaye A. B., Handler G., Krisciunas K., Poretti E., Zerbi F. M., 1999, PASP, 111, 840

Lampens P., Frémat Y., Vermeylen L., De Cat P., Dumortier L., Sódor Á., Sharka M., et al., 2018, BSRSL, 87, 137

Lampens P., Vermeylen L., De Cat P., Sodór Á., Bógnar Z., Frémat Y., Skarka M., et al., 2020, svos.conf, 353

Lenz P., Breger M., 2005, CoAst, 146, 53

Poro A., Paki E., Mazhari G., Sarabi S., Kahraman Alicavus F., Ahangarani Farahani F., Guilani H., et al., 2021, PASP, 133, 084201. doi:10.1088/1538-3873/ac12dc

Ricker G. R., Winn J. N., Vanderspek R., Latham D. W., Bakos G. Á., Bean J. L., Berta-Thompson Z. K., et al., 2015, JATIS, 1, 014003. doi:10.1117/1.JATIS.1.1.014003

Rodríguez, E. & Breger, M. 2001, Astron. and Astrophys. , 366, 178. doi:10.1051/0004-6361:20000205

Stassun K. G., Oelkers R. J., Paegert M., Torres G., Pepper J., De Lee N., Collins K., et al., 2019, AJ, 158, 138. doi:10.3847/1538-3881/ab3467

Uytterhoeven K., Moya, A., Grigahcène A., Guzik, J. A., Gutiérrez-Soto, J., et al., 2011, A&A, 534, AA125

Table 1. Results of the frequency analysis. Harmonic and combination frequencies are not given in this list. The full list of the frequencies is given in electronic form.

	TIC 25537276				TIC 177422294				
	Frequency (d^{-1})	Amplitude (mmag)	Phase (rad)	S/N		Frequency (d^{-1})	Amplitude (mmag)	Phase (rad)	S/N
ν_1	7.55054 ± 0.00002	8.872 ± 0.008	0.2364 ± 0.0001	534.6	ν_1	8.30240 ± 0.00016	6.863 ± 0.006	0.0739 ± 0.0011	14
ν_2	8.03904 ± 0.00008	2.237 ± 0.008	0.6364 ± 0.0006	151.0	ν_2	7.66622 ± 0.00036	3.318 ± 0.006	0.0640 ± 0.0026	6.6
ν_3	7.37013 ± 0.00011	1.739 ± 0.008	0.3471 ± 0.0007	107.3	ν_3	7.07205 ± 0.00039	3.208 ± 0.006	0.5485 ± 0.0028	6.1
ν_4	5.78908 ± 0.00012	1.506 ± 0.008	0.6576 ± 0.0008	100.5	ν_4	8.204374 ± 0.00028	4.808 ± 0.006	0.918 ± 0.002	9.9
ν_5	7.04380 ± 0.00026	0.706 ± 0.008	0.1234 ± 0.0018	43.8	ν_5	8.23038 ± 0.00015	2.438 ± 0.006	0.033 ± 0.001	8.7
ν_6	7.57891 ± 0.00062	0.321 ± 0.008	0.0344 ± 0.0044	19.2	ν_6	8.12435 ± 0.00081	2.438 ± 0.006	0.0852 ± 0.0064	5.0
ν_7	15.0991 ± 0.00110	0.168 ± 0.008	0.8044 ± 0.0078	14.3	ν_7	4.51330 ± 0.00048	2.551 ± 0.06	0.8588 ± 0.0034	5.3
ν_8	7.65999 ± 0.00474	0.103 ± 0.008	0.9871 ± 0.0337	6.3	ν_8	7.70823 ± 0.00042	2.723 ± 0.006	0.5254 ± 0.0031	5.4
ν_9	7.94174 ± 0.00177	0.111 ± 0.008	0.4499 ± 0.0126	7.3	ν_9	8.39643 ± 0.000224	2.929 ± 0.006	0.3438 ± 0.0016	6.4
ν_10	8.00864 ± 0.00554	0.101 ± 0.008	0.4312 ± 0.0395	6.6	ν_10	5.23151 ± 0.00056	2.272 ± 0.006	0.9086 ± 0.0041	5.1

	TIC 252554307				TIC 279874050				
	Frequency (d^{-1})	Amplitude (mmag)	Phase (rad)	S/N		Frequency (d^{-1})	Amplitude (mmag)	Phase (rad)	S/N
ν_1	7.57891 ± 0.00003	5.213 ± 0.008	0.3055 ± 0.0002	288.6	ν_1	12.85860 ± 0.00032	9.709 ± 0.001	0.3965 ± 0.1035	62.6
ν_2	7.51810 ± 0.00003	0.565 ± 0.008	0.2651 ± 0.0002	313.5	ν_2	11.55165 ± 0.00003	4.149 ± 0.005	0.0212 ± 0.0024	29.7
ν_3	8.07147 ± 0.00015	0.132 ± 0.008	0.6219 ± 0.00107	77.4	ν_3	12.86759 ± 0.00016	5.091 ± 0.001	0.3965 ± 0.0081	32.8
ν_4	7.45324 ± 0.00010	0.174 ± 0.008	0.8083 ± 0.0007	99.1	ν_4	12.69569 ± 0.00026	2.476 ± 0.001	0.0211 ± 0.0081	28.4
ν_5	7.39851 ± 0.00012	0.125 ± 0.006	0.2630 ± 0.0025	70.6	ν_5	12.89069 ± 0.00015	2.438 ± 0.006	0.2630 ± 0.0025	14.7
ν_6	8.00458 ± 0.00053	0.237 ± 0.008	0.006 ± 0.2702	89.8	ν_6	12.90520 ± 0.00039	2.375 ± 0.006	0.2702 ± 0.0046	15.4
ν_7	5.76070 ± 0.00018	0.953 ± 0.008	0.5921 ± 0.0013	54.9	ν_7	12.84552 ± 0.00054	1.608 ± 0.004	0.7985 ± 0.0052	10.1
ν_8	7.68634 ± 0.00015	0.122 ± 0.008	0.2223 ± 0.0010	66.8	ν_8	11.58353 ± 0.00065	1.327 ± 0.0042	0.7832 ± 0.0054	9.2
ν_9	7.00933 ± 0.00066	0.262 ± 0.008	0.72455 ± 0.0047	14.9					
ν_10	7.79377 ± 0.00054	0.144 ± 0.008	0.1784 ± 0.0038	8.16					

Table 1. Continuation.

	TIC 308447073				TIC 367910480			
	Frequency (d^{-1})	Amplitude (mmag)	Phase (rad)	S/N	Frequency (d^{-1})	Amplitude (mmag)	Phase (rad)	S/N
ν_1	3.39196 ± 0.00003	1.820 ± 0.008	0.9407 ± 0.0007	104.8	15.6652 ± 0.00003	0.516 ± 0.008	0.5253 ± 0.0025	22.8
ν_2	3.57380 ± 0.00040	4.641 ± 0.008	0.5525 ± 0.0026	30.7	4.04676 ± 0.00002	0.464 ± 0.006	0.0212 ± 0.0023	8.4
ν_3	3.71073 ± 0.00015	0.358 ± 0.008	0.1172 ± 0.0035	21.3	6.10102 ± 0.00004	0.438 ± 0.007	0.3323 ± 0.0034	10.9
ν_4	3.43462 ± 0.00010	0.380 ± 0.007	0.5469 ± 0.0039	21.4	19.87434 ± 0.00004	0.379 ± 0.007	0.4481 ± 0.0028	21.7
ν_5	3.35380 ± 0.00012	0.318 ± 0.006	0.2343 ± 0.0044	18.1	3.64199 ± 0.00004	0.340 ± 0.006	0.8268 ± 0.0031	6.3
					2.59348 ± 0.00004	0.298 ± 0.006	0.3935 ± 0.0035	6.1
					3.34585 ± 0.00004	0.285 ± 0.006	0.0536 ± 0.0037	5.1
					3.34585 ± 0.00004	0.285 ± 0.006	0.0536 ± 0.0037	5.1
					3.54846 ± 0.00003	0.275 ± 0.006	0.0332 ± 0.0039	4.9
					5.76989 ± 0.00005	0.245 ± 0.006	0.3817 ± 0.0043	5.3

	TIC 370599803				TIC 395520454			
	Frequency (d^{-1})	Amplitude (mmag)	Phase (rad)	S/N	Frequency (d^{-1})	Amplitude (mmag)	Phase (rad)	S/N
ν_1	18.32261 ± 0.00009	3.664 ± 0.001	0.9809 ± 0.0006	84.5	2.82490 ± 0.00052	1.924 ± 0.006	0.5297 ± 0.0009	44.1
ν_2	9.19831 ± 0.00010	3.507 ± 0.001	0.5446 ± 0.0007	51.8	2.76637 ± 0.00118	1.870 ± 0.003	0.9027 ± 0.0009	42.5
ν_3	9.80307 ± 0.00015	2.270 ± 0.001	0.6731 ± 0.0011	36.1	3.06876 ± 0.00016	1.363 ± 0.001	0.0541 ± 0.0012	31.7
ν_4	9.86653 ± 0.00010	1.948 ± 0.001	0.1550 ± 0.0013	30.5	2.56933 ± 0.00015	0.261 ± 0.006	0.8112 ± 0.0025	5.9
ν_5	12.63869 ± 0.00012	1.509 ± 0.006	0.35997 ± 0.0016	23.5	2.56933 ± 0.00015	0.261 ± 0.006	0.3928 ± 0.0025	14.7
ν_6	8.72465 ± 0.00053	1.256 ± 0.001	0.9525 ± 0.0019	5.7	3.38871 ± 0.00092	0.229 ± 0.001	0.0258 ± 0.0068	15.4
ν_7	10.05893 ± 0.00018	1.207 ± 0.001	0.3085 ± 0.0020	18.6	2.98097 ± 0.00102	2.186 ± 0.001	0.0258 ± 0.0072	5.5
ν_8	10.92167 ± 0.00015	0.121 ± 0.008	0.0247 ± 0.0020	25.7	6.14338 ± 0.00132	1.858 ± 0.001	0.0336 ± 0.0093	9.2
ν_9	13.64733 ± 0.00066	8.735 ± 0.008	0.0247 ± 0.0028	6.8				
ν_10	11.41436 ± 0.00054	0.826 ± 0.008	0.3125 ± 0.0029	16.04				

Table 1. Continuation.

	TIC 400502454				TIC 431375592			
	Frequency (d^{-1})	Amplitude (mmag)	Phase (rad)	S/N	Frequency (d^{-1})	Amplitude (mmag)	Phase (rad)	S/N
ν_1	6.59953 ± 0.00007	3.398 ± 0.001	0.4157 ± 0.0005	112.2	4.86512 ± 0.00005	19.915 ± 0.009	0.0034 ± 0.0007	756.6
ν_2	5.93556 ± 0.000132	2.003 ± 0.001	0.8206 ± 0.0009	57.9	2.43893 ± 0.00014	2.912 ± 0.009	0.0833 ± 0.0002	56.2
ν_3	3.71104 ± 0.00011	1.192 ± 0.001	0.0247 ± 0.0015	26.8	2.39483 ± 0.00024	1.902 ± 0.009	0.9105 ± 0.0003	36.3
ν_4	7.95496 ± 0.00011	0.907 ± 0.001	0.9105 ± 0.0015	43.3	2.37720 ± 0.00033	0.907 ± 0.009	0.56145 ± 0.0006	17.2
ν_5	1.35331 ± 0.00011	0.598 ± 0.001	0.4110 ± 0.0030	10.1				
ν_6	9.64449 ± 0.00011	0.581 ± 0.001	0.4577 ± 0.0031	21.6				
ν_7	4.68162 ± 0.00011	0.468 ± 0.001	0.6521 ± 0.0038	10.8				
ν_8	0.66185 ± 0.00011	0.346 ± 0.001	0.2089 ± 0.0052	5.2				